Potential evaluation of bio-oil production through catalytic pyrolysis of forest biomass

Ameixa, Marcelo[1]

Instituto Superior Técnico, Universidade de Lisboa, Avenida Rovisco Pais, 1049-001 Lisboa, Portugal

ABSTRACT

This dissertation consisted in the study of forest biomass, particularly biomass from *pinus pinaster* and *eucalyptus globulus*.

The thermogravimetry trials enabled us to obtain the quantity of lignocellulosic components and analyse the thermic decomposition to calculate the kinetics parameters. The obtained lignocellulosic compounds were 36% and 40% of hemicellulose, 21% and 15% of cellulose and 25% and 21 % of lignin for pine and eucalyptus respectively. The kinetics parameters were calculated for pine trunk and eucalyptus leaves through Kissinger Flynn-Wall-Ozawa (FWA) and Kissinger-Akahira-Sunode (KAS) methods. The biomass sample were also analysed through Fourier transformed infrared (FTIR) spectroscopy, here it was seen that the eucalyptus fruits and leaves show a very different composition for the rest of the biomass.

The pyrolysis trials were made with different biomass mixes for various times and temperature, with or without catalyst. The eucalyptus pyrolysis at 425 ºC produced a higher quantity of bio-oil, 48%, the pyrolysis duration did not affect each product yield, the catalysts mainly favoured the gasification except for marble which enhanced the bio-oil production. The produced bio-oils were analysed by thermogravimetry to find which had the highest volatile amount (mass loss T<325ºC). The bio-oil was also characterized by FTIR spectroscopy to identify the different functional groups present (mainly aromatics, alkanes and carboxylic acids).

Keywords: Bio-oil, pyrolysis, forest waste, thermogravimetry, FTIR, catalysis.

1 INTRODUCTION

Energy demand is rapidly increasing since it is a vital part of the world's development and economic growth [1] [2]. This growth can be observed in Figure 1, the world's primary energy supply in 2015 more than doubled the one in 1971. Unfortunately, most of this demand is fulfilled by fossil fuels, a non-renewable energy resource heavily related with greenhouse gas emission [1] [2]. The increasing energy consumption plus finite fossil fuel resources lead to a cumulative increase in greenhouse gas emissions and in fossil fuel cost, which promote the research on renewable energy sources [3].

Lignocellulosic biomass is an abundant renewable source of energy and a promising feedstock to produce chemicals, fibers, plastics and other commodities originally obtained using petroleum, and since it is not part of the

[1] Corresponding author.
E-mail address: marcelo.ameixa@ist.utl.pt

human food chain its use does not jeopardize the world's food supply [4] [5]. It can be transformed through different thermal, physical and biological process, and among this processes pyrolysis, the thermal decomposition in an oxygen-free environment is one of the most interesting and is used commercially [6] [7]. The pyrolysis products, bio-oil, bio-char and non-condensable gases, yields and composition differ depending on biomass composition, reaction condition and catalyst type [8].

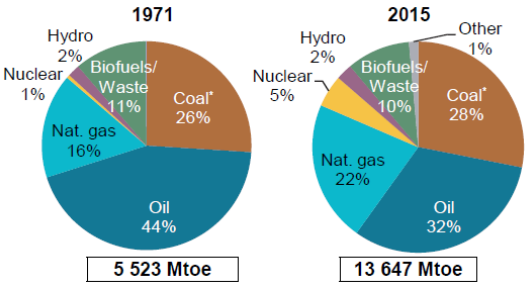

Figure 1 - Total primary energy supply by fuel in millions of tonnes of oil equivalent. Adaptation of [6].

2 MATERIALS AND METHODS

2.1 FOREST BIOMASS

The raw material for this work was wood wastes from Portuguese forest (Table 1). The samples were collected, ground and then stored, without humidity control.

2.2 THERMOGRAVIMETRY

The biomass and bio-oil thermogravimetry (TG) were conducted using a TG-DTA/DSC Sateram labsys using appropriate software. To introduce the samples in the equipment it was used an alumina crucible.

The biomass TG were carried out in an air atmosphere and in a nitrogen atmosphere, while the bio-oil was only run with an air atmosphere. The flux of both gases was adjusted with a Brooks Instrument mass flow controller Model 5878, and escape into the atmosphere.

2.3 KINETIC ANALYSIS

The kinetics parameters can be obtained from the TG, this work will focus on Kissinger, Flynn-Wall-Ozawa (FWO), and Kissinger-Akahira-Sunode (KAS) methods.

The Kissinger method uses the linearization of Equation 1 to obtain the activation energy, Ea, and the pre-exponential factor from the Arrhenius equation, A.

In Equation 1 β represents the highest weight loss rate, T_{max} the temperature which correspond to the highest weight loss, R is the gas constant and $f'(\alpha_{max})$ is the derivative function of Šesták e Berggren general Equation 2 [9] [10].

For kinetics analysis of the thermic decomposition of biomass is usually considered a first order reaction, n=1, and typically m=p=0 [11].

This method's hindrance is only resulting in a set of kinetic parameters for each TG trial, which does not reflect the results for complex materials.

This method's hindrance is only resulting in a set of kinetics parameters for each TG trial, which does not reflect the results for complex materials.

The FWO method is described by Equation 3, where β_i represents weight loss rate, Ea_α, the activation energy at α, conversion, A_α is the pre-exponential factor from the Arrhenius equation at α, T_α is the temperature at which α is obtained, and g(α) is the symmetric Napierian logarithm of 1-α [10].

The last method applied was KAS method, which is described by Equation 4 [10].

The obtained values can be related with the ones in the literature for each compound, these values are discriminated in Table 2.

.

$$\ln\left(\frac{\beta}{T_{max}^2}\right) = -\frac{Ea}{RT_{max}} + \ln\left(-\frac{AR}{Ea}f'(\alpha_{max})\right) \quad (1)$$

$$f(\alpha) = \alpha^m(1-\alpha)^n[-\ln(1-\alpha)]^p \quad (2)$$

$$\ln(\beta_i) = -1{,}052\frac{Ea_\alpha}{RT_\alpha} + \ln\left(\frac{A_\alpha Ea_\alpha}{g(\alpha)R}\right) - 5.331 \quad (3)$$

$$\ln\left(\frac{\beta_i}{T_\alpha^2}\right) = -\frac{Ea_\alpha}{RT_\alpha} + \ln\left(\frac{A_\alpha \mathrm{R}}{\mathrm{g}(\alpha) Ea_\alpha}\right) \quad (4)$$

Table 1 – Biomass samples identification

ID	Tree	Section
BM1	Pine	Trunk
BM2	Pine	Trunk
BM3	Pine	Leaves
BM4	Pine	Branch
BM5	Pine	Leaves
BM6	Eucalyptus	Fruits
BM7	Eucalyptus	Twig
BM8	Eucalyptus	Fruits
BM9	Eucalyptus	Leaves
BM10	Pine	Twig
BM11	Pine	Branch
BM12	Eucalyptus	Twig
BM13	Eucalyptus	Trunk
BM14	Pine	Twig
BM15	Pine	Trunk
BM16	Eucalyptus	Twig
BM17	Eucalyptus	Bark
BM18	Eucalyptus	Twig
BM19	Eucalyptus	Trunk
BM20	Eucalyptus	Bark
BM21	Pine	Branch
Pine	Pine	All [(a)]
Eucalyptus	Eucalyptus	All [(b)]
Fruits	Eucalyptus	Fruits [(c)]
Leaves	Eucalyptus	Leaves
BMmix	Pine + Eucalyptus	All [(d)]

Table 2 - Activation energy for lignocellulosic compounds [12].

	Hemicellulose	Cellulose	Lignin
Ea (kJ/mol)	80-116	195-286	18-65

2.4 FTIR

The FTIR trials were conducted using a horizontal attenuated total reflectance equipment, Perkin-Elmer Spectrum Two FT-IR Spectrometer, with an ATR accessory with a ZnSe crystal; this procedure was applied to the biomass BM1 to BM21 and the bio-oils obtained through pyrolysis. For BM2, BM3, BM11, and BM19 it was made 16 scans, for the rest of the biomass samples it was 8 scans and for the bio-oil 4 scans, all with 4 cm-1 resolutions.

The obtained spectra were corrected using Kubelka-Munk function (equation 5), where R is the reflectance and I the intensity. This method decreases the noise in the results.

$$I_{corrected} = \frac{(1-R)^2}{2R} \quad (5)$$

2.5 PYROLYSIS

The pyrolysis trials occurred in a laboratory installation with a fixed bed vertical reactor installed in a temperature controlled cylindrical hoven, from Eurotherm, with an inert atmosphere of nitrogen 99,5%. It is important to mention that for these trials only the Pine, Eucalyptus, Leaves, Fruit and BMmix biomass were used.

The reactor consists of a cylindrical glass column, in which it is inserted glass wool in its bottom extremity, above a layer of inert material (silicon carbide, SiC) with more glass wool on top, and finally the biomass; the installation also includes a condenser, after the reactor, inserted in water. During pyrolysis the liquid product is withheld in the inert material to be recovered using an appropriate solvent, in this case acetone, the incondensable gas leaves the installation with the nitrogen to the atmosphere, while the condensable ones stay in the condenser to be also removed with the assistance of an appropriate solvent. The bio-char stays in where the biomass once was, above the superior glass wool.

3 RESULTS AND DISCUSSION

3.1 BIOMASS

3.1.1 THERMOGRAVIMETRY

All TG studies were performed for various parts of pine and eucalyptus it was decided to do the average for each tree to see the differences between the species, this comparison is represented in Figure 2.

The water content in both trees is almost the same, which does not happen with the hemicellulose curve since it is unnoticeable in the pine biomass.

3.1.2 KINETIC ANALYSIS

The kinetics analysis was performed for pine trunk and eucalyptus leaves, for this study it was realized five TG trials (5, 10, 25, 35 and 45 º). The kinetics analysis data is summarized in Table 3 to Table 5. The eucalyptus leaves present two distinct points of high weight loss per minute, so it was decided to apply Kissinger method to both values. The pine activation energy (Ea) is close to the lower end of cellulose Ea, this may happen because of hemicellulose degrades at similar temperatures than cellulose in pine trees. The eucalyptus leaves activation energy increases with the conversion that can be explained by the oils it is known to carry.

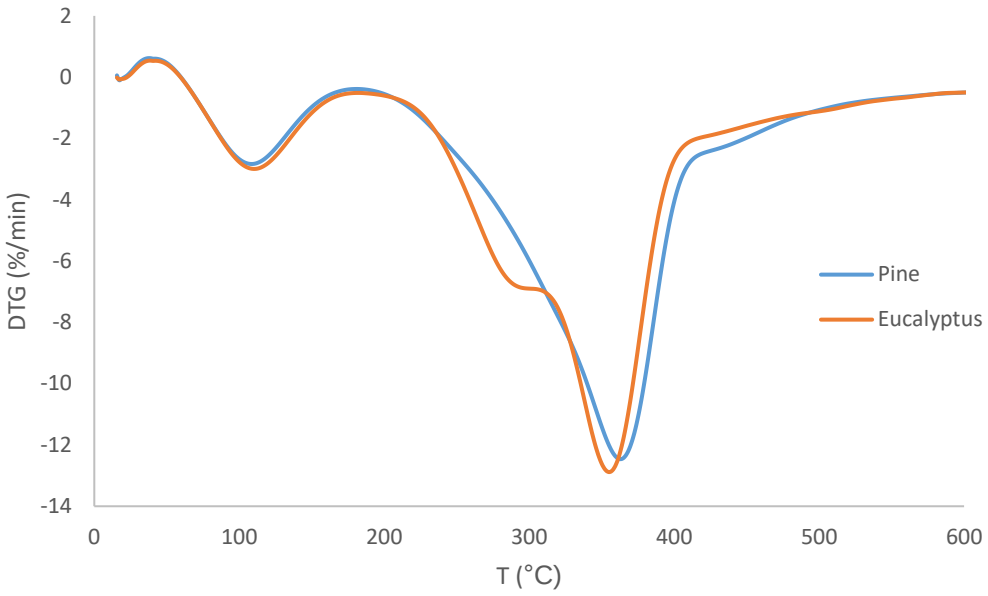

Figure 2 - Average DTG curve of each tree over temperature with a heating rate of 25 °C/min

Table 3 - Kinetic parameters and linear correlation coefficient obtained using Kissinger method.

	BM1	BM6.1	BM6.2
Ea (kJ/mol)	162	257	135
A (s^{-1})	$1{,}1 \times 10^{13}$	$5{,}9 \times 10^{21}$	$6{,}6 \times 10^{12}$
R^2	0,999	0,992	0,989

Table 4 - Kinetic parameters and linear correlation coefficient obtained using FWO method

α	BM1			BM6		
	Ea (kJ/mol)	**A (s^{-1})**	**R^2**	**Ea (kJ/mol)**	**A (s^{-1})**	**R^2**
0,1	174	$7{,}0 \times 10^{14}$	0,92	144	$3{,}4 \times 10^{13}$	0,99
0,2	184	$1{,}6 \times 10^{15}$	0,98	197	$1{,}7 \times 10^{18}$	0,99
0,3	189	$2{,}2 \times 10^{15}$	0,99	327	$3{,}1 \times 10^{28}$	0,98
0,4	172	$5{,}2 \times 10^{13}$	0,99	383	$3{,}1 \times 10^{31}$	0,89
0,5	169	$2{,}0 \times 10^{13}$	0,97	412	$4{,}9 \times 10^{28}$	0,79

Table 5 - Kinetic parameters and linear correlation coefficient obtained using KAS method.

α	BM1			BM6		
	Ea (kJ/mol)	A (s^{-1})	R^2	Ea (kJ/mol)	A (s^{-1})	R^2
0,1	174	$6{,}8 \times 10^{14}$	0,92	143	$2{,}7 \times 10^{13}$	0,99
0,2	184	$1{,}5 \times 10^{15}$	0,98	199	$2{,}3 \times 10^{18}$	0,99
0,3	189	$2{,}0 \times 10^{15}$	0,99	334	$3{,}3 \times 10^{28}$	0,98
0,4	170	$3{,}7 \times 10^{13}$	0,99	392	$1{,}2 \times 10^{32}$	0,89
0,5	167	$1{,}3 \times 10^{13}$	0,97	421	$1{,}5 \times 10^{29}$	0,78

3.1.3 FTIR

The different biomass samples were also analyzed through FTIR to obtain qualitative information about its compounds, the results are in Figure 3

From Figure 3 it is noticeable that the highest value for each biomass, 1032-1017 cm^{-1}, is roughly the same which corresponds to C-O valence vibration (cellulose and hemicellulose).

Using the data in Table 6, it is possible to identify the other maximums as well with enface to wavelength 1603 cm^{-1} that is an aromatic skeletal vibration plus C=O stretching (lignin), 1440 cm^{-1} is an O–H in plane deformation (lignin), 1370-1365 cm^{-1} is an aliphatic C–H stretch in CH3; not in O–Me (lignin), 1310 cm^{-1} is a CH_2 wagging (cellulose and hemicellulose), 1235-1225 cm^{-1} is a C–C plus C–O plus C=O stretch (cellulose), 1205–1200 cm^{-1} is an OH plane deformation (cellulose and hemicellulose) and 858–853 cm^{-1} C–H out-of-plane (lignin). .

Table 6 - Functional groups and component identifiable classes in the FTIR spectrum for biomass.

Wavelength (cm^{-1})	Functional group	Components	Reference
1603	Aromatic skeletal vibration + C=O stretching	Lignin	[13]
1440	O-H plane deformation	Lignin	[14]
1370-1365	Aliphatic C-H stretching in CH_3; not methanol	Lignin	[15]
1310	CH_2 wagging	Cellulose and hemicellulose	[14]
1235-1225	C-C + C-O + C=O stretch	Cellulose	[15]
1205-1200	O-H plane deformation	Cellulose and hemicellulose	[15]
1047-1004	C-O valence vibration	Cellulose and hemicellulose	[15]
858-853	C-H out of plane	Lignin	[15]

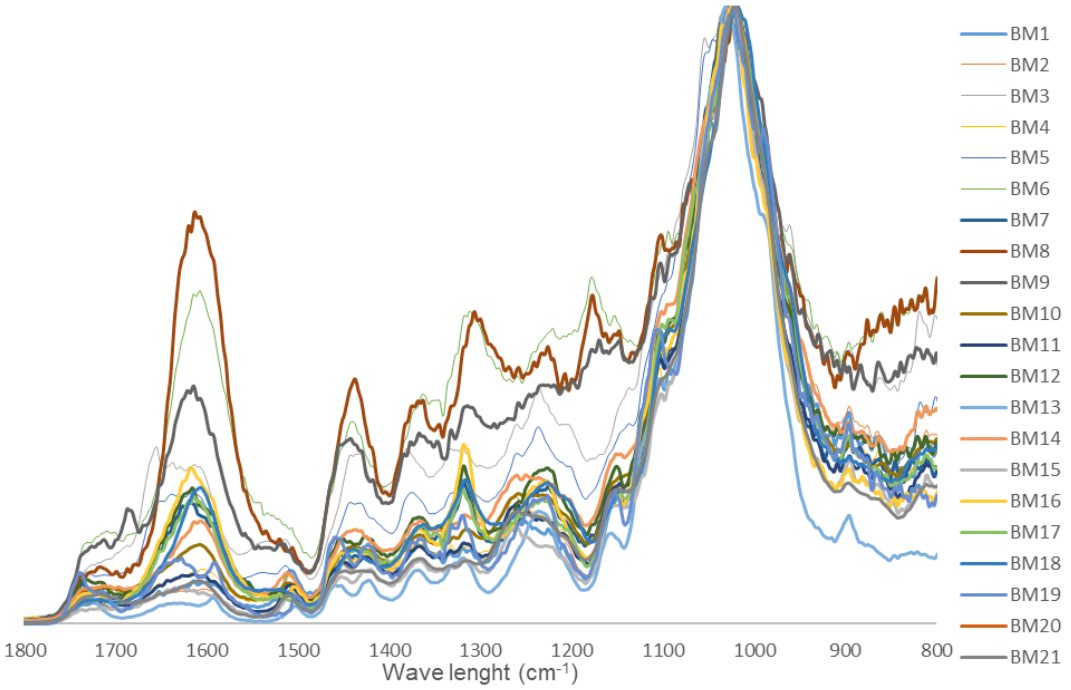

Figure 3- Biomass FTIR spectrum between 1800 and 800 cm^{-1}

3.2 PYROLYSIS

3.2.1 PYROLYSIS YIELD

The pyrolysis trials objective was to quantify the yields of, bio-char, bio-oil, and gases the trials with and without catalyst can be found in Figure 4.The only catalyst that rose the bio-oil yield was marble, bauxite kept a similar bio-oil yield, increasing the gas output at Bio-char's expense. The CaO presents the highest gas yield of 48% and the lowest yield produced. The bio-char was weighted after every trial, the bio-oil was obtained through evaporation of the liquid obtained in a rotary evaporator and the wet gas was calculated with the other two yields. The different conditions and yields obtained for each trial can be found in Table 7. The representation of of bio-char. zeolite Y, zeolite β, and sodium carbonate show similar yields that in comparison with the catalyst-free trial present lower bio-oil rates resulting in higher gas yields.

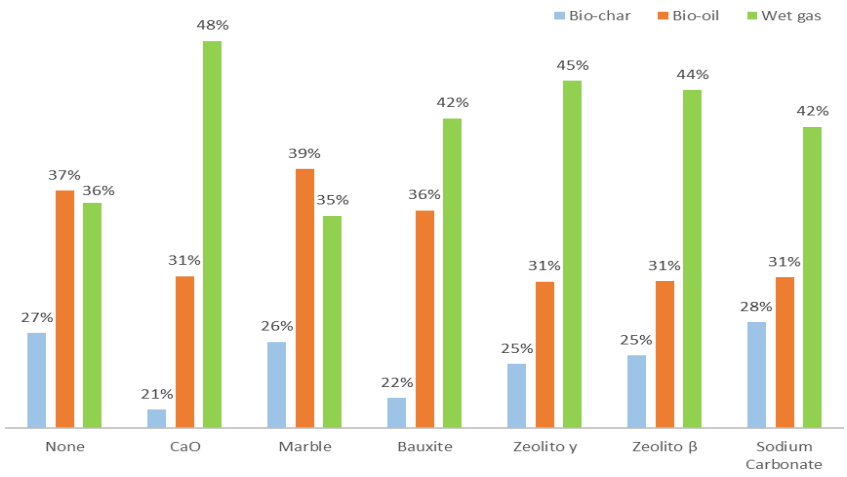

Figure 4 - Pyrolysis yields of BMmix for 10-minute trials at 425 °C with and without a catalyst

Table 7 - Pyrolysis conditions and resulting yields

Biomass	m (g)	T (ºC)	t (min)	Catalyst	m_{cat} (g)	Bio-char (%wt.)	Bio-oil (%wt.)	Wet gas (%wt)
Pine	10,03	375	10	-	0	36	37	27
Pine	10,02	425	10	-	0	30	30	40
Pine	10	500	10	-	0	27	38	35
Eucalyptus	10,03	375	10	-	0	33	35	32
Eucalyptus	10,15	425	10	-	0	27	44	30
Eucalyptus	10	500	10	-	0	24	37	39
Fruits	10	425	10	-	0	42	25	33
Leaves	10,02	425	10	-	0	30	35	35
BMmix	10,03	375	10	Sodium Carbonate	2,01	33	25	42
BMmix	10,04	400	10	-	0	28	44	28
BMmix	10	400	10	Sodium Carbonate	2,02	31	24	45
BMmix	10,01	425	5	-	0	26	36	38
BMmix	10,02	425	10	-	0	27	38	36
BMmix	10,02	425	10	-	0	27	39	34
BMmix	10,04	425	10	-	0	27	36	37
BMmix	10,01	425	10	-	0	27	36	37
$BMmix_{Av}$	10,02	425	10	-	0	27	37	36
BMmix	10,02	425	10	CaO	2	21	31	48
BMmix	10	425	10	Marble	2,05	26	39	35
BMmix	10,01	425	10	Bauxite	2,04	22	36	42
BMmix	10	425	10	Zeolite y	2	25	31	45
BMmix	9,99	425	10	Zeolite β	2	25	31	44
BMmix	10,01	425	10	Sodium Carbonate	2,05	28	31	42
BMmix	10,05	425	15	-	-	26	36	38

3.2.2 THERMOGRAVIMETRY

The thermogravimetry analysis was used to characterize the bio-oils behavior with a heat flux of 20 °C/min under an air atmosphere. The DTG results for the bio-oil produced using different catalysts in 10-minute trials at 425 °C are represented in Figure 5. It is noticeable that the addition of a catalyst produces a higher quantity of volatile compounds and with their amount increase also increases the temperature at which they present a higher weight loss. Excluding the trial for the bio-oil produced using sodium carbonate, that presents a lower temperature for the maximum weight loss rate than the one obtained from the uncatalyzed pyrolysis, but this one presents an irregularity in the beginning of the trial, unfortunately, it was not possible to repeat due to equipment malfunction.

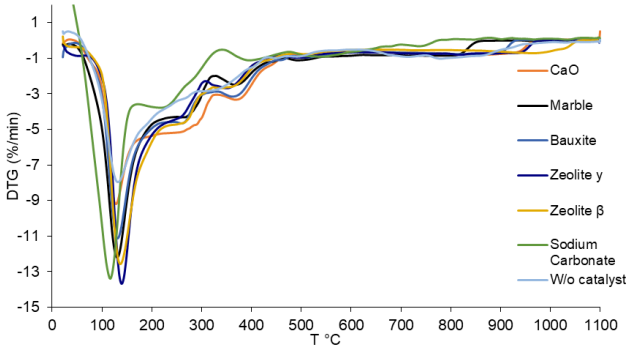

Figure 5 - DTG curves for BMmix bio-oil produced with different catalysts.

3.2.3 FTIR

For a better understanding of the bio-oil composition, it was applied the FTIR spectroscopy technique, each spectrum was divided in two for an easier observation, the first part shows the spectrum from a wavelength of 1800 to 600 cm^{-1} and the second part from 3700 to 2500 cm^{-1}. Through observation of Table 9 is possible to conclude that zeolite Y reduces the C=O stretching functional group in the bio-oil, while sodium carbonate seems to produce more C=O since every other group losses amplitude. The CaO also shows an increase in alkenes, between 1150 and 1000 cm^{-1}.

Table 8 - Functional groups and component identifiable classes in the FTIR spectrum for bio-oil [35].

Wavelength (cm^{-1})	Functional group	Components
3500-3200	O-H stretching	Polymeric O-H, water impurities
3050-2800	C-H stretching	Alkanes
1750-1650	C=O *stretching*	Aldehydes, ketones, carboxylic acids, quinones, etc.
1645-1500	C=C *stretching*	Alkenes
1475-1350	C-H bending	Alkanes
1300-1150	C-O stretching	Primary, secondary and tertiary alcohols
1300-1150	O-H *bending*	Phenols, esters and ethers
1150-1000	C-H bending	Alkenes
900-675	O-H bending	Aromatic compounds

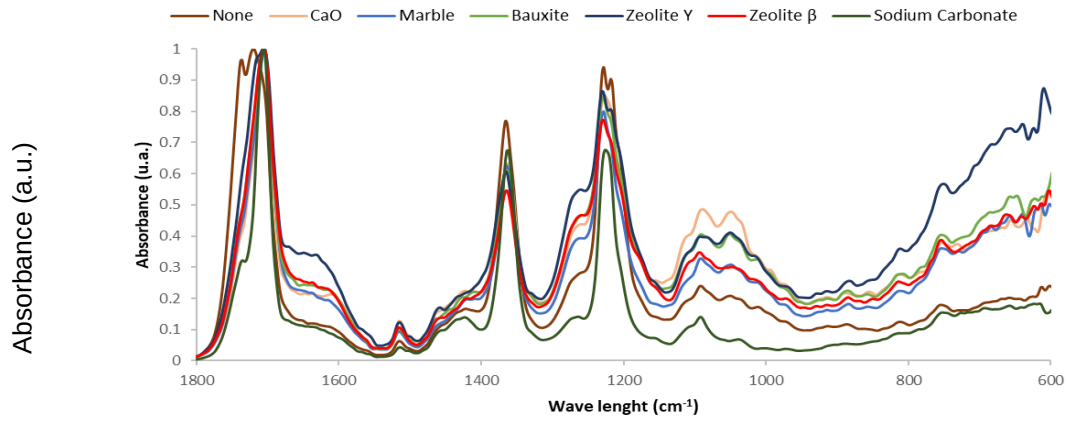

Figure 6 - FTIR spectrum of catalytic and non-catalytic pyrolysis bio-oil from 1800 to 600 cm-1.

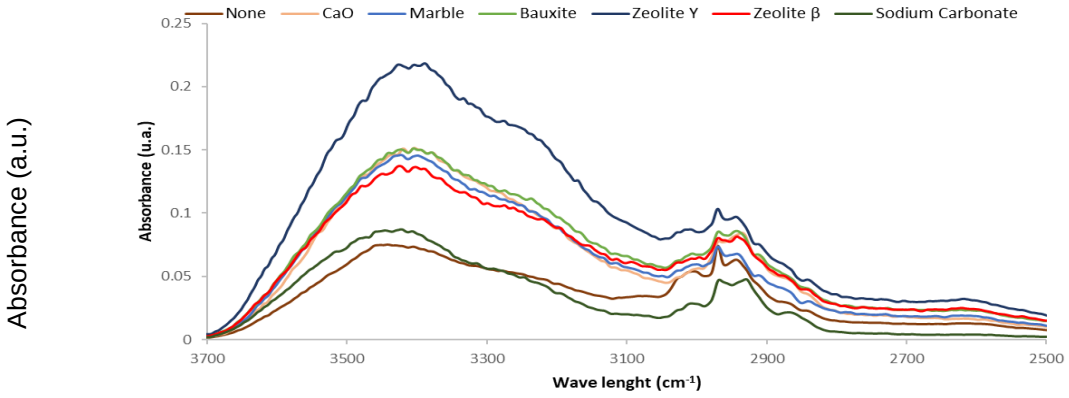

Figure 7 - FTIR spectrum of catalytic and non-catalytic pyrolysis bio-oil from 3700 to 2500 cm-1.

4 CONCLUSION

Woody wastes biomass from Portuguese forest can be used to produce renewable fuels with the advantage of simultaneous decrease of wild fires occurrence.

Twenty one samples of biomasses from *pinus pinaster* and *eucalyptus globulus* were characterized by thermogravimetry and used in a fixed bed pyrolysis reactor to produces bio-gas, bio-oil and bio-char. Despite the differences in lignocellulosic compositions the pyrolysis yields were similar for all the analyzed samples, with exception of eucalyptus leaves and fruits because they contained appreciable amounts of oils.

The use of alkali and alkali earths carbonates as pyrolysis catalysts improves the wet gas yield and ameliorate the bio-oil quality. Waste from ornamental stone industry such as powdered marble showed interesting performances as pyrolysis catalysts, promoting higher bio-oil yield with simultaneous improvement of its composition.

5 BIBLIOGRAPHY

[1] A. M. &. M. Y. Qazi Sohaib, "Fast pyrolysis of sugarcane bagasse: Effect of pyrolysis conditions on final product distribution and properties," *Energy Sources, Part A: Recovery, Utilization, and Environmental Effects,* pp. 184-190, 2017.

[2] L. C. J. G.-Q. F. V. M. H. A. Marcilla, "A review of thermochemical conversion of microalgae," *Renewable and Sustainable Energy Reviews,* vol. 27, pp. 11-19, 2013.

[3] M. A. A. K. G. A. O. M. j. Jemaa Mabrouki, "Simulation of biofuel production via fast pyrolysis of palm oil residues," *Fuel,* 2015.

[4] C. (. X. R. P. M. L. N. M. Luana Dessbesell, "Forest biomass supply chain optimization for a biorefinery aiming to produce high value bio-based materials and chemicals from lignin and forestry residues: A review of literature," 2016.

[5] P. Basu, Biomass Gasification and Pyrolysis: Pratical Design and Theory, Oxford, UK: Elsevier Inc., 2010.

[6] C. V. A. B. a. J. M. E. J. L. Figueiredo, "Pyrolysis of holm-oak wood: influence of temperature and particle size," *Fuel,* vol. 68, pp. 1012-1016, 1989.

[7] Y. L. K. C. M. L. H. L. B. L. Dengyu Chen, "Pyrolysis polygeneration of poplar wood: Effect of heating rate and pyrolysis temperature," *Bioresource Technology,* vol. 218, pp. 780-788, 2016.

[8] H. T. Vamshi Krishna Guda, "Altering bio-oil composition by catalytic treatment of pine wood pyrolysis vapors over zeolites using an auger - packed bed integrated reactor system," *Biofuel,* vol. 11, pp. 448-457, 2016.

[9] J. Š. a. G. Berggren, "Study of the kinetics of the mechanism of solid-state reactions at increasing temperature.," *Thermochimica Acta,* vol. 3, pp. 1-12, 1971.

[10] A. K. B. J. M. L. A.-M. C. P. N. S. Sergey Vyazovkin, "ICTAC Kinetics Committee recommendations for performing kinetic computations on thermal analysis data," *Thermochimica Acta,* vol. 520, pp. 1-19, 2011.

[11] J. M. J. S. a. H. T. Nobuyoshi Koga, "Data Treatment in Non-isothermal Kinetics and Diagnostic Limits of Phenomenological Models," *Netsu Sokutei,* vol. 4, pp. 213-223, 1993.

[12] C. D. Blasi, "Modeling chemical and pyrolysis processes of wood and biomass pyrolysis," *Progress in Energy and Combustion Science,* vol. 34, pp. 47-90, 2010.

[13] S. K. a. J. F. Kadla, "Hydrogen Bonding in Lignin: A Fourier Transform Infrared Model Compound Study," *Biomacromolecules,* vol. 6, pp. 2815-2821, 2005.

[14] J. M. G. Deborah L. Sills, "Using FTIR to Predict Saccharification From Enzymatic Hydrolysis of Alkali-Pretreated Biomasses," *Biotechnology Bioengineering,* vol. 109, pp. 353-362, 2011.

[15] J. R. H. P. B. H. M. Schwanninger, "Effects of short-time vibratory ball milling on the shape of FT-IR spectra of wood and cellulose," *Vibrational Spectroscopy,* vol. 36, pp. 23-40, 2004.